eLIFE elifesciences.org

RESEARCH ARTICLE

Figures and figure supplements

A tissue-specific, Gata6-driven transcriptional program instructs remodeling of the mature arterial tree

Marta Losa *et al*

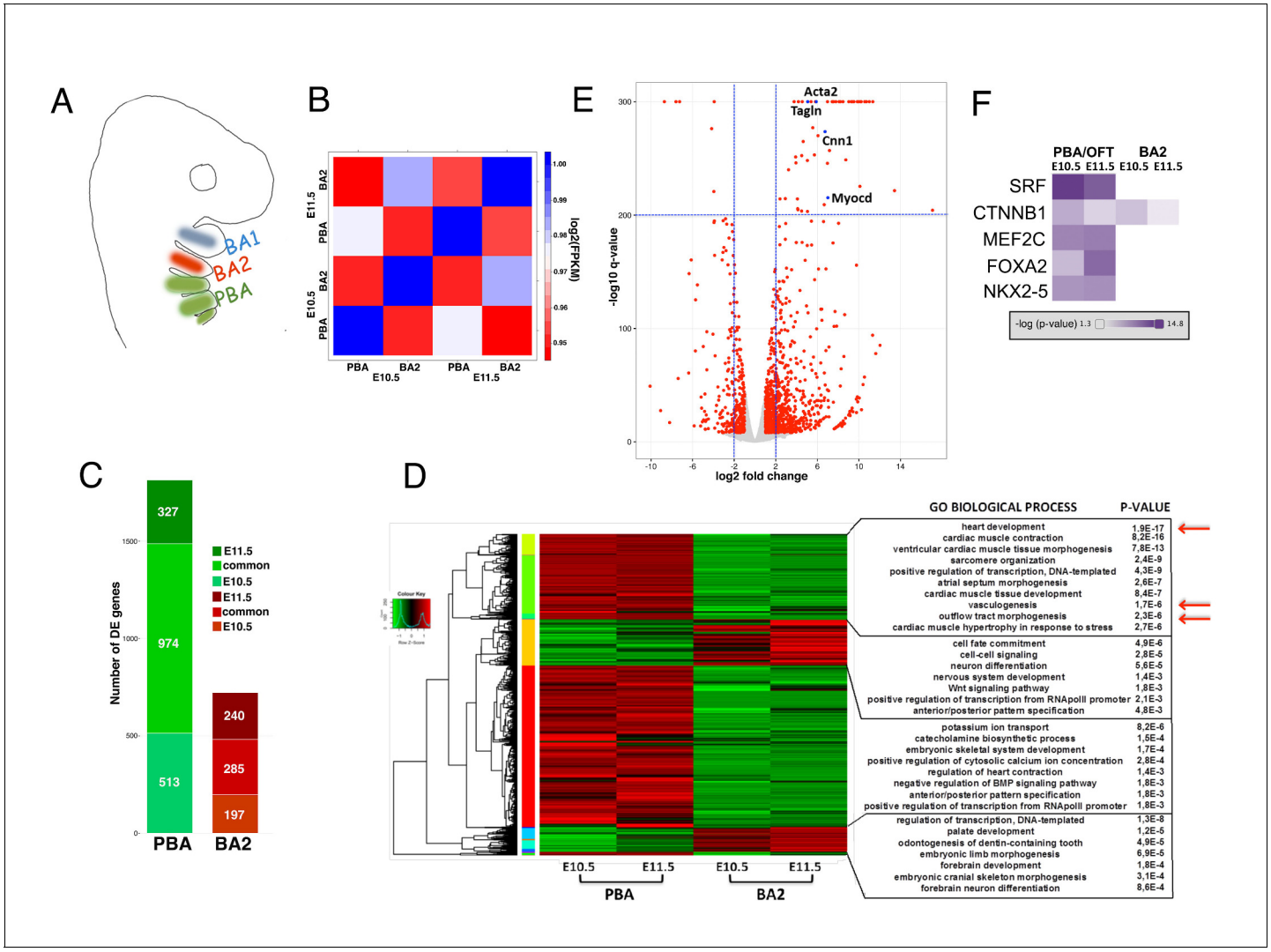

Figure 1. Global transcriptomes of developing BAs and OFT. (**A**) In mammals, BA2 (red) hosts aortic arch (AA)2, which regresses, while posterior BAs (PBA, green) host AA3-6, which contribute to the main thoracic arteries. (**B**) Correlation plot of global expression profiling separates BA2 and PBA at E10.5 and E11.5. Heatmap shows the Spearman correlation coefficients for each pair of samples based on the normalized expression values (FPKM). (**C**) Count of DE genes between PBA and BA2 (fold change ≥±2; q-value <0.05) at E10.5–11.5. The bar plot shows PBA/OFT-enriched genes as the largest fraction of DE genes (color-coded as in A). (**D**) Hierarchical clustering of DE genes in any of the three pair-wise comparisons. DAVID analysis (***Huang et al., 2009***) of the clusters generated detects significant association with PBA/OFT-specific Biological Process GO terms (arrows). (**E**) Volcano plot. Top significant PBA/OFT-enriched genes are highly expressed in SMCs. (**F**) Ingenuity Pathway Analysis (IPA) identifies the TF SRF as the most likely upstream regulator of PBA/OFT-enriched genes (p-value<1e-20). SRF targets include *Myocd* and known Myocd targets (e.g. *Acta2*, *Tagln*).

DOI: https://doi.org/10.7554/eLife.31362.002

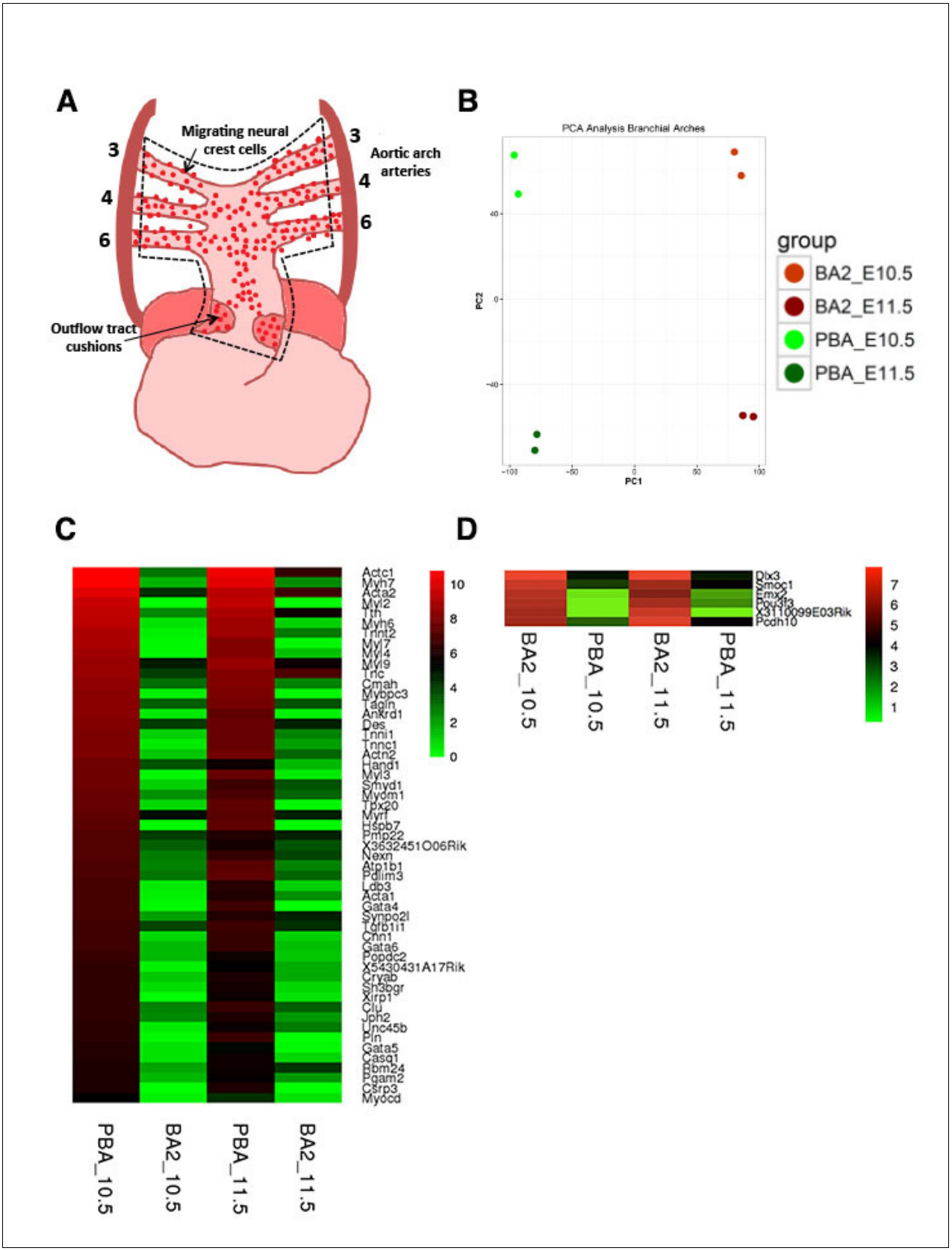

Figure 1—figure supplement 1. Differential expression across developing BAs. (**A**) Embryonic circulation, front view (adapted from ***High and Epstein, 2008***). The broken line encloses the PBA/OFT, the embryonic area used as a source of RNA. The AA3, 4 and 6 are housed by BA3-6 (PBA in green in

Figure 1—figure supplement 1 continued on next page

Figure 1—figure supplement 1 continued

Figure 1A) (**B**) PCA shows reproducibility of the biological replicates and separates BA2 and PBA/OFT at both developmental stages. (**C–D**) Heatmaps of top significant DE genes (Volcano plot in ***Figure 1***, upper right and left quadrants) in PBA/OFT (**C**) and BA2 (**D**).

DOI: https://doi.org/10.7554/eLife.31362.003

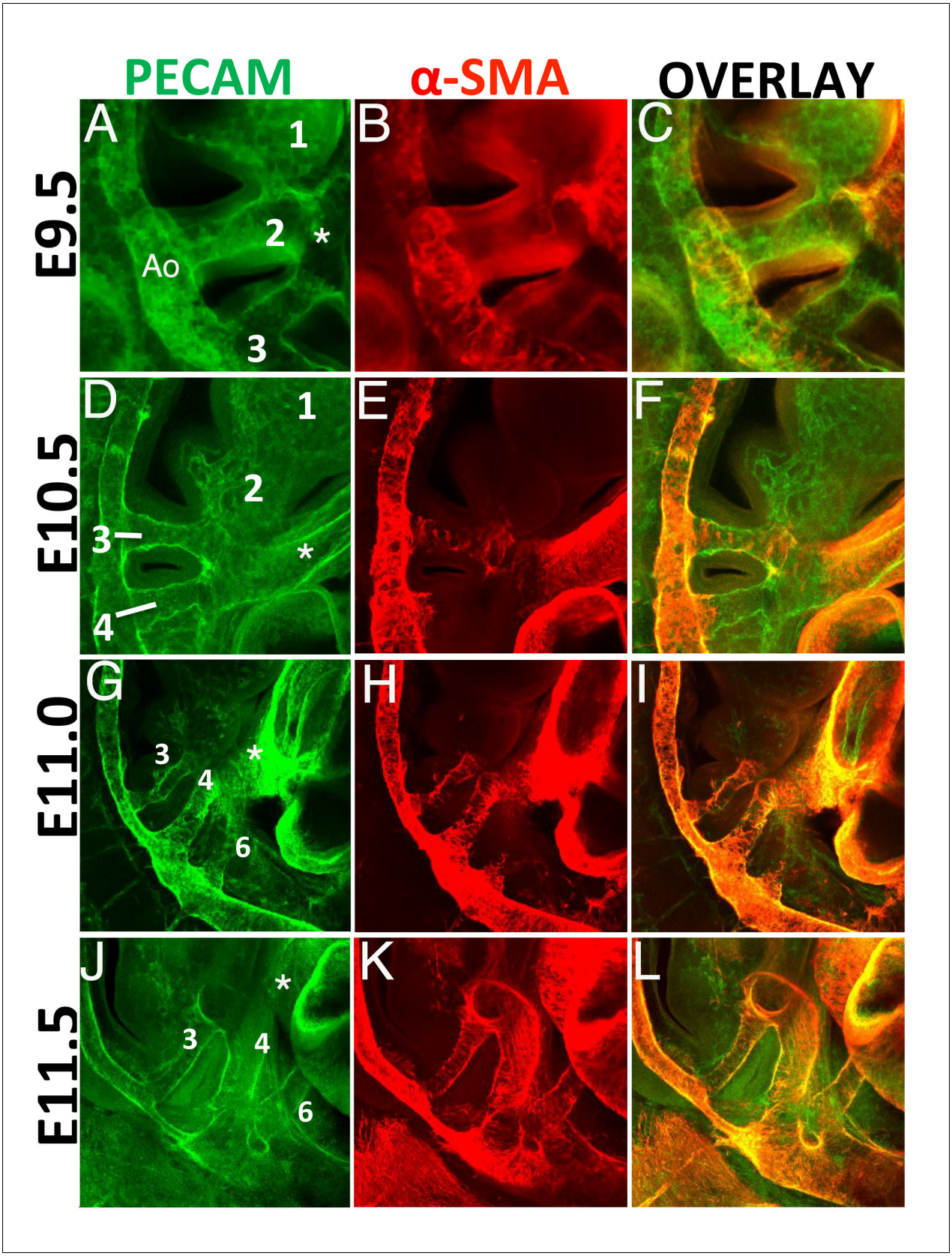

Figure 2. SMCs are generated exclusively in BA3-6, in a rostro-caudal fashion. Confocal analysis of whole mount wild type embryos at E9.5 (**A–C**), E10.5 (**D–F**), E11.0 (**G–I**) and E11.5 (**J–L**) to visualize the endothelial network (PECAM, green) (**A,D,G, J**) and vascular SMCs (SMA, red) (**B, E, H, K**). C, F, I, L are

Figure 2 continued on next page

Figure 2 continued

overlays of PECAM and SMA staining. (**A-C**) At E9.5 (25 somites, (**s**), AAs 2 and 3 are connected to the dorsal aorta. AA1 has already started to regress into capillary beds. SMA-positive cells are visible in the dorsal aorta and OFT, but are not detected in the walls of AA2-3. (**D–F**) At E10.5 (37s), AA3 and AA4 are fully formed, but only AA3 is associated to vascular SMCs. Capillary beds replace AA2 in BA2. G-I. A clear AA6 is visible at E11.0 (43s). At this stage AA3-4 are fully covered with SMA-positive cells, while the newly formed AA6 is not associated with vascular SMCs. (**J–L**) At E11.5 (48s) formation of AA3, 4 and 6 is complete. All visible AAs (AA3-4-6) are covered by SMA-positive cells. Right view. Ao, aorta; asterisks label the OFT.

DOI: https://doi.org/10.7554/eLife.31362.004

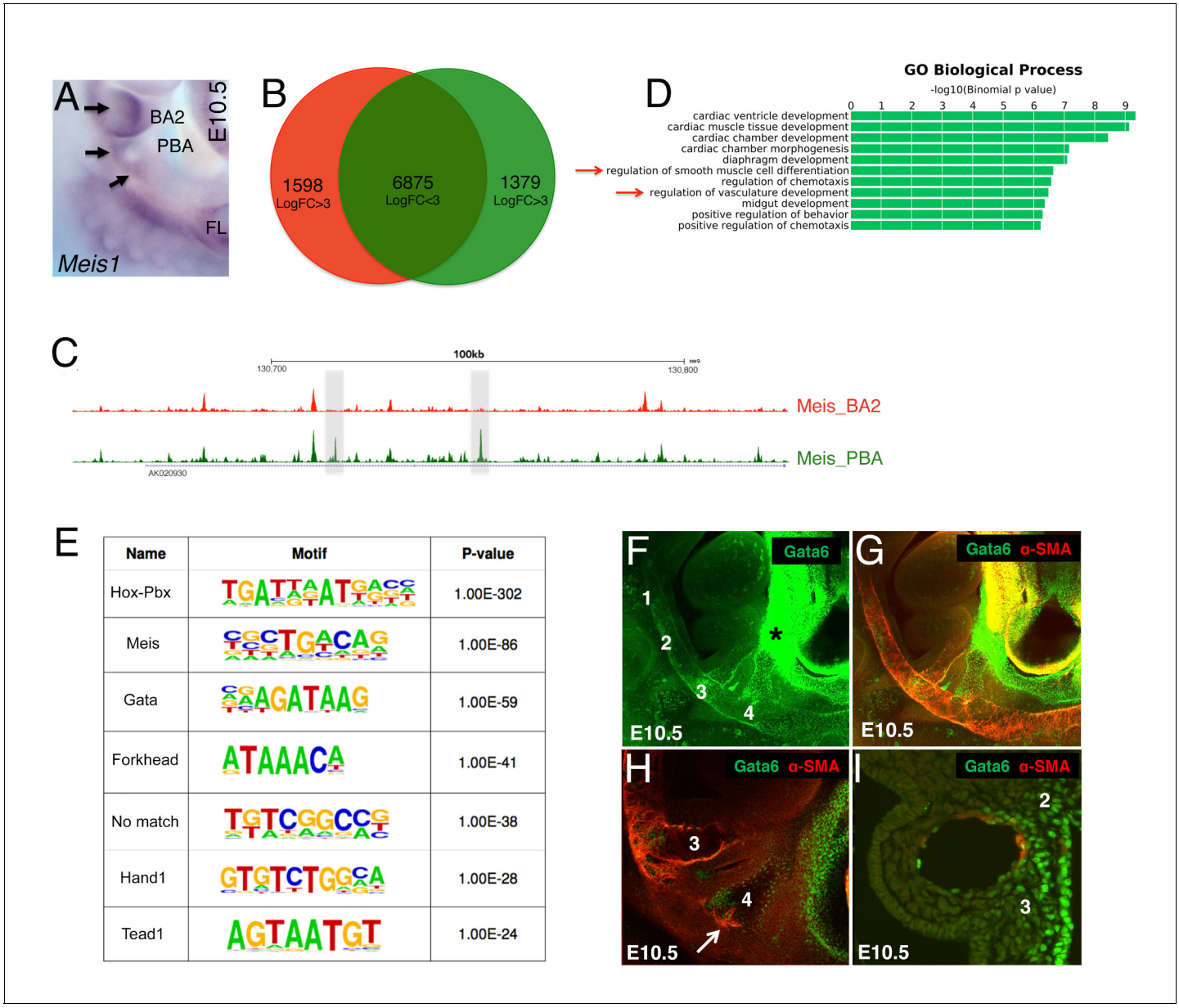

Figure 3. Unbiased identification of main TFs instructing PBA-specific transcription. (**A**) Whole mount in situ hybridizations on E10.5 mouse embryo. *Meis1* is expressed in the BA2 (arrow) and in the PBA (BA3 and BA4, arrows). (**B**) Diffrep analysis of Meis binding in PBA and BA2. Venn diagram shows 'shared' Meis binding sites (FE $\geq$ 10) with logFC < 3 signal (n = 6875) and with higher (logFC $\geq$ 3) signal in PBA (green) and BA2 (red). (**C**) UCSC browser tracks upstream of *Nrp1* illustrate the largely overlapping binding of Meis in PBA and BA2, with instances of increased Meis binding signal (gray regions) in PBA relative to BA2. (**D**) Top over-represented biological processes associated to Meis peaks (FE $\geq$ 10) with higher signal in PBA (logFC $\geq$ 3) include 'smooth muscle cell differentiation' and 'vasculature development'. (**E**) De novo motif discovery on Meis peaks (FE $\geq$ 10) with higher signal in PBA identifies high enrichment of the recognition sequence for GATA TFs, together with motifs recognized by Meis and Meis partners Hox/Pbx. (**F–I**) Confocal analysis of E10.5 embryos (36–37 s) whole mount (**F–H**) and sagittal sections (**I**) stained with Gata6 (**F**) and Gata6/SMA antibodies (**G–I**). Gata6 is detected in the BA3, BA4 (**F–H**) and the heart region (**F–G**). Individual z-stack (**H**) shows Gata6 co-localization with SMA-positive cells in the BA3 and the appearance of SMCs in Gata6-positive area in the BA4 (arrow). Gata6/SMA-positive cells surround AA3 (**I**). Numbers indicate corresponding BAs; asterisks label the OFT.

DOI: https://doi.org/10.7554/eLife.31362.005

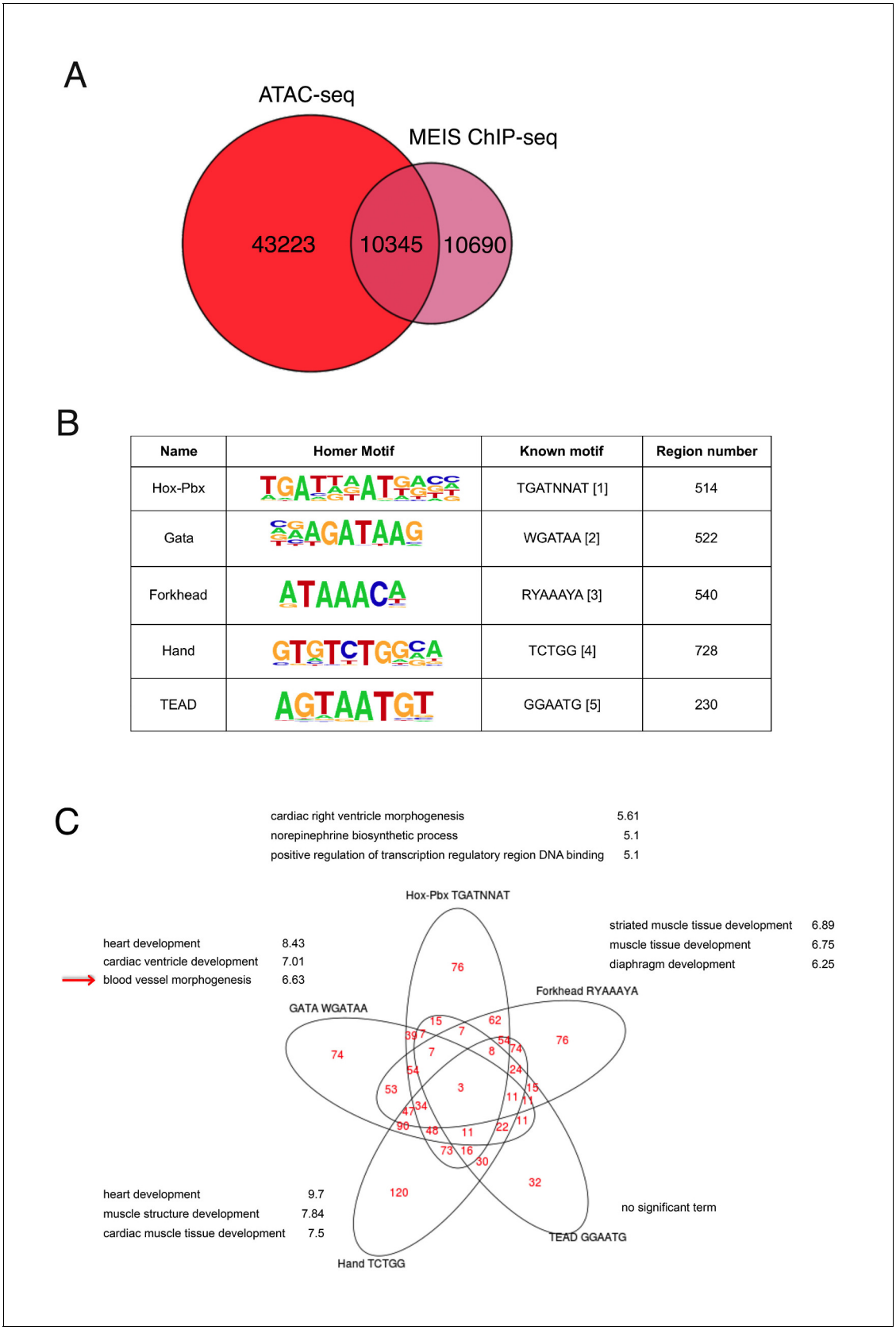

Figure 3—figure supplement 1. Analysis of Meis-bound regions containing different TF recognition motifs. (**A**) Comparison of Meis ChIP-seq (FE ≥ 10 peaks) in E11.5 BA2 and ATAC-seq in E10.5 BA2. Half of Meis peaks overlap with accessible chromatin in the BA2. (**B**) Experimentally identified motifs

Figure 3—figure supplement 1 continued on next page

Figure 3—figure supplement 1 continued

(known motifs), which correspond to Homer identified motifs, were used to count the instances of highly enriched (logFC <3)Meis binding (200nt summit regions, FE $\geq$ 10) containing at least one motif. (**C**) Functional enrichment of motifs regions (-log10 p-value) and their intersections. Venn diagram shows the intersection of Meis-bound regions containing each motif and their corresponding top three GO biological processes. In Meis regions containing GATA motifs, the term 'muscle development' did not appear in the full list. 'Blood vessel morphogenesis' was also associated to Forkhead-containing regions. TEAD- containing regions did not return any significant term. 1. (***Donaldson et al., 2012***); 2. (***Han et al., 2016***); 3. (***Nakagawa et al., 2013***); 4. (***Hollenberg et al., 1995***); 5. (***Diepenbruck et al., 2014***).

DOI: https://doi.org/10.7554/eLife.31362.006

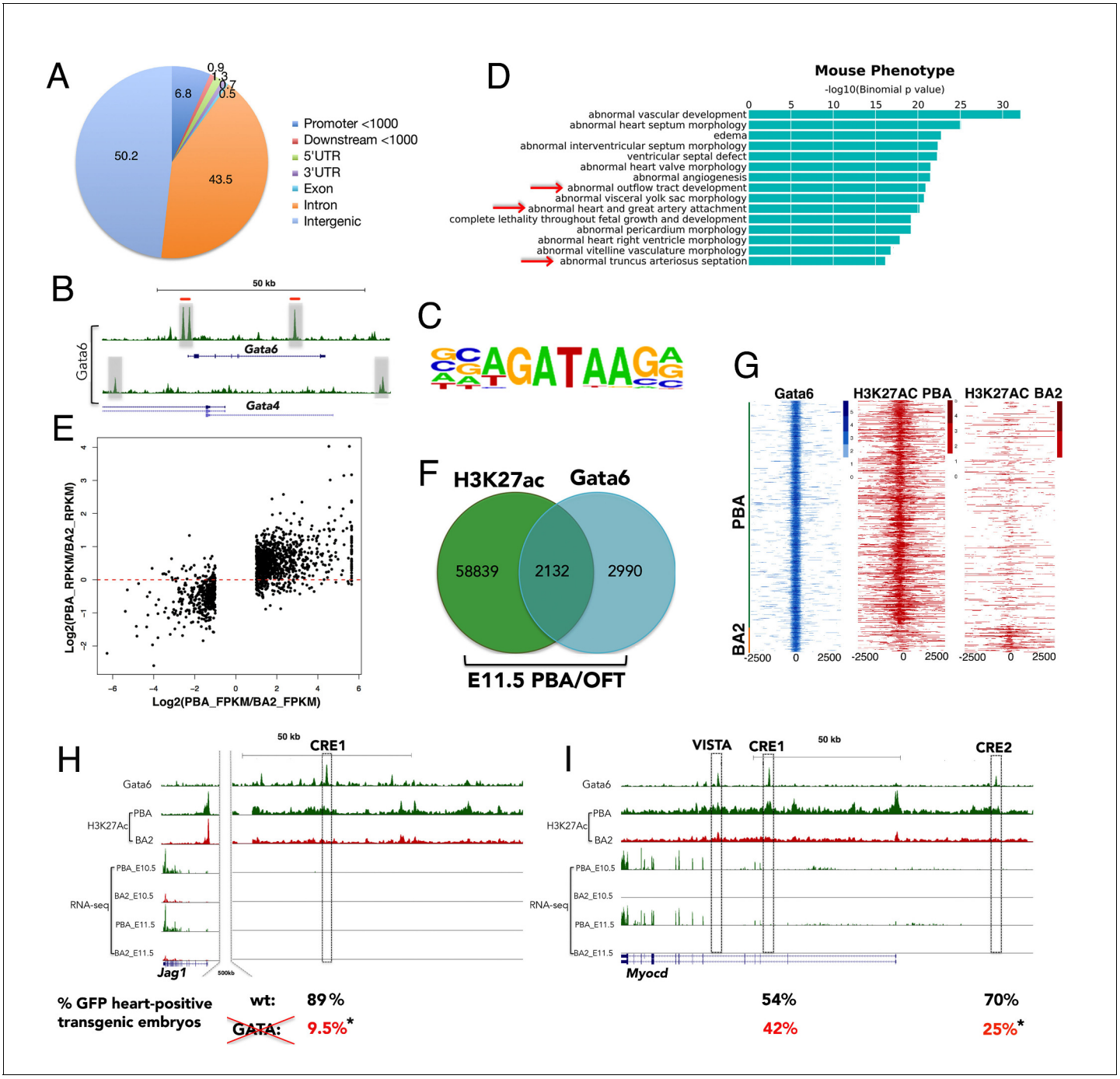

Figure 4. Gata6 occupies active enhancers in PBA/OFT. (**A**) CEAS analysis of the distribution of Gata6 peaks relative to Reference Sequence (RefSeq) gene structures. The pie chart and corresponding percentage values indicate the proportion of reads. (**B**) UCSC browser tracks shows Gata6 binding (gray regions) at *Gata4* and *Gata6* loci. Red lines indicate Gata4 binding in E12.5 ventricles. (**C**) Sequence logo of the most significant motifs identified using de novo motif discovery. (**D**) Top over-represented mouse phenotypes associated to Gata6 peaks. The x axes values correspond to the binomial raw (uncorrected) p-values. (**E**) Scatterplot of the Log2(ratio of FPKM) values for DE genes between PBA and BA2 versus the Log2(ratio of RPKM) values of their H3K27ac signals at promoters and distal regions (Correlation: 0.694; p<2.2e-16). (**F**) Venn diagram (not proportional) of Gata6 peaks (200nt summits) and H3K27Ac-positive regions in the PBA/OFT. Almost half of Gata6 peaks overlap regions acetylated in the PBA/OFT. (**G**) Heatmap of Gata6 peaks and corresponding H3K27ac peaks (within 5000 nt of the summit) shows most Gata6 peaks overlap PBA/OFT-specific enhancers (n = 820), and only a minority of BA2-specific enhancers (n = 98). Regions detected as H3K27Ac-positive in both PBA/OFT and BA2 were excluded from this analysis. (**H, I**) UCSC browser tracks. RNA-seq and ChIP-seq profiles for Gata6 binding and H3K27Ac in the PBA/OFT and H3K27Ac in the BA2 at *Jag1* (**H**) and *Myocd* (**I**) loci. Gata6 binds regions highly acetylated in PBA/OFT, but not BA2 (boxed; VISTA highlights a heart-positive enhancer). Numbers

Figure 4 continued on next page

Figure 4 continued

correspond to the % of embryos injected with wild-type (upper row, in black) and mutant (lower row, in red) enhancers, displaying reporter activity in the heart in addition to the midbrain (positive control); asterisks denote p-value<0.05 (Fisher's Exact Test).

DOI: https://doi.org/10.7554/eLife.31362.007

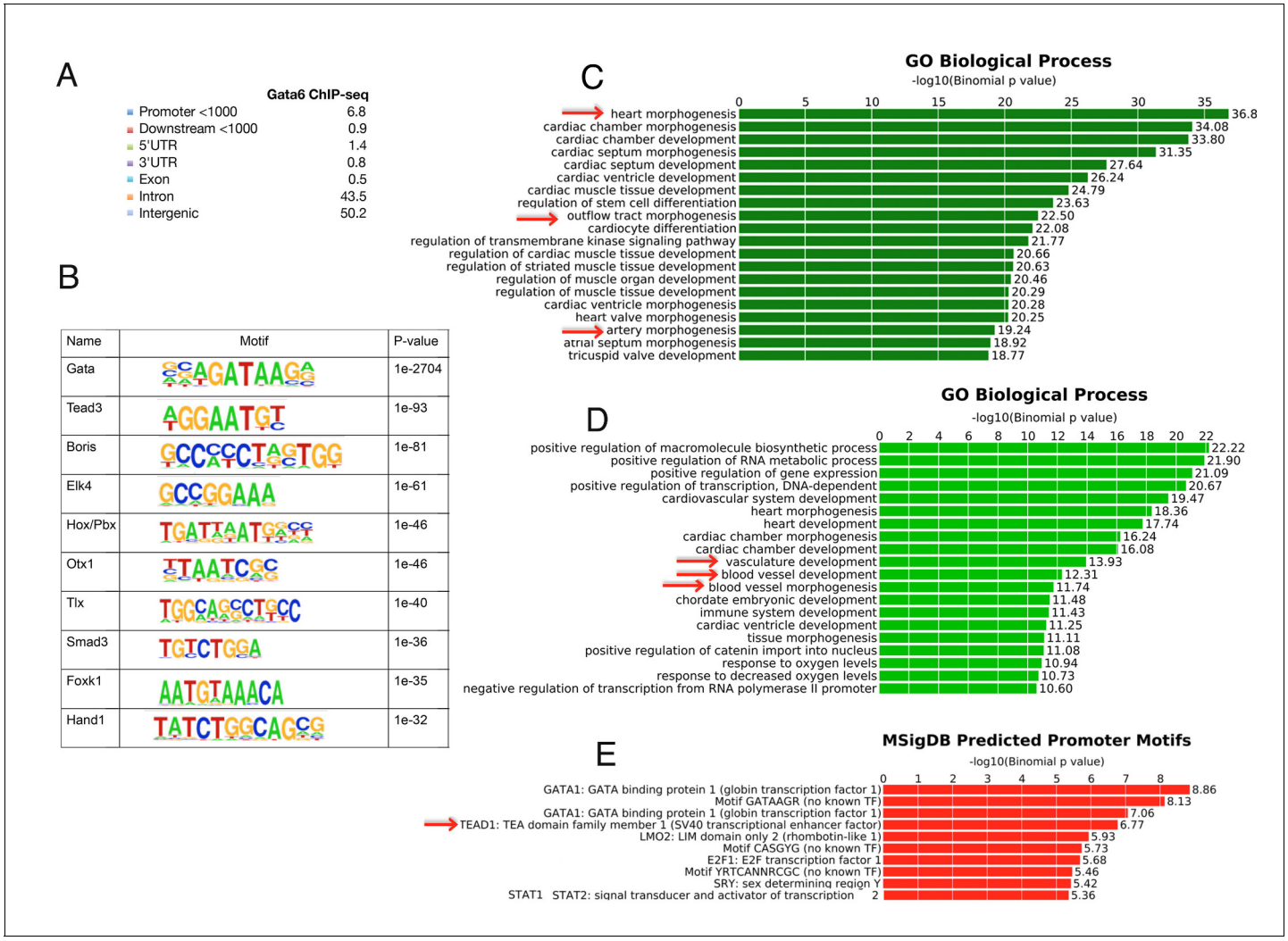

Figure 4—figure supplement 1. Extended analysis of Gata6 peaks. (**A**) CEAS analysis of the distribution of Gata6 peaks relative to Reference Sequence (RefSeq) gene structures. Numbers correspond to percentage values; the proportion of reads is shown in the pie chart In ***Figure 4A***. (**B**) Sequence logo of motifs identified by Homer. (**C**) Top over-represented biological processes associated to Gata6 peaks. The x axes values correspond to the binomial raw (uncorrected) p-values. (**D**) Top over-represented biological processes associated to PBA/OFT-specific enhancers bound by Gata6 (n = 820). (**E**) Predicted motifs in promoters associated to PBA/OFT-specific enhancers bound by Gata6 (n = 820).

DOI: https://doi.org/10.7554/eLife.31362.008

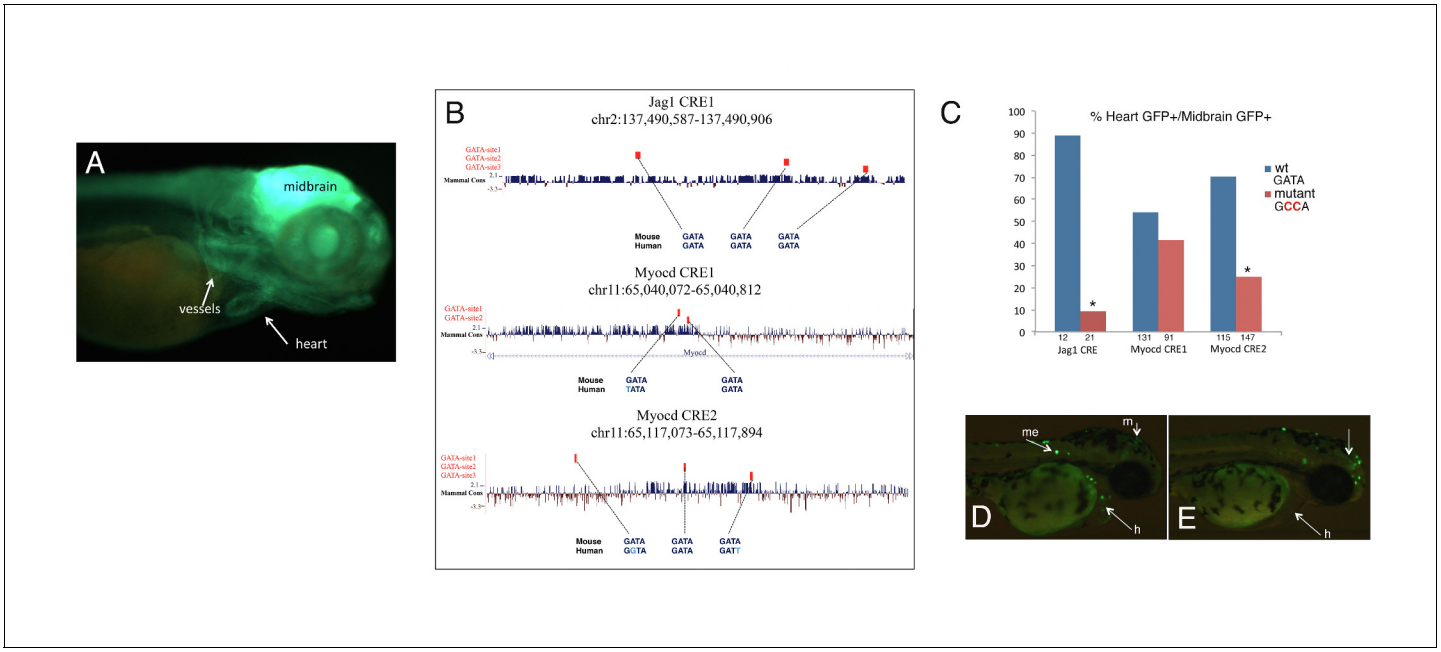

Figure 4—figure supplement 2. Disrupting GATA motifs affects the activity of GATA6-bound enhancers. (**A**) GFP reporter activity in Myocd CRE1 lines. Lines were derived from embryos injected with Myocd CRE1. Myocd CRE1 drives GFP in the heart and in vessels-like structures. The construct also contains a control enhancer, which drives GFP activity in the midbrain. (**B**) Genomic coordinates (mm9) and nucleotide sequence of the regions injected in zebrafish. The overall mammal conservation is shown, together with the sequence conservation and position of the GATA motifs. In mutant enhancers, each GATA was replaced by GCCA. (**C**) Activity of the wild-type (blue) and corresponding mutant (red) enhancers expressed as percentage of midbrain GFP-positive embryos (positive control) also showing GFP expression in the heart. For each wild-type and mutant enhancer, numbers on the x axis correspond to the total number of midbrain-positive embryos; asterisks denote p-value<0.05 (Fisher's Exact Test: Myocd CRE1 p-value=0.07686; Myocd CRE2 p-value=1.838e-13; Jag1 CRE: p-value=3.978e-05). (**D, E**) GFP reporter activity in embryos injected with wild-type (H) and mutant (I) *Jag1* CRE1. M, midbrain; me, melanocytes; h, heart.

DOI: https://doi.org/10.7554/eLife.31362.009

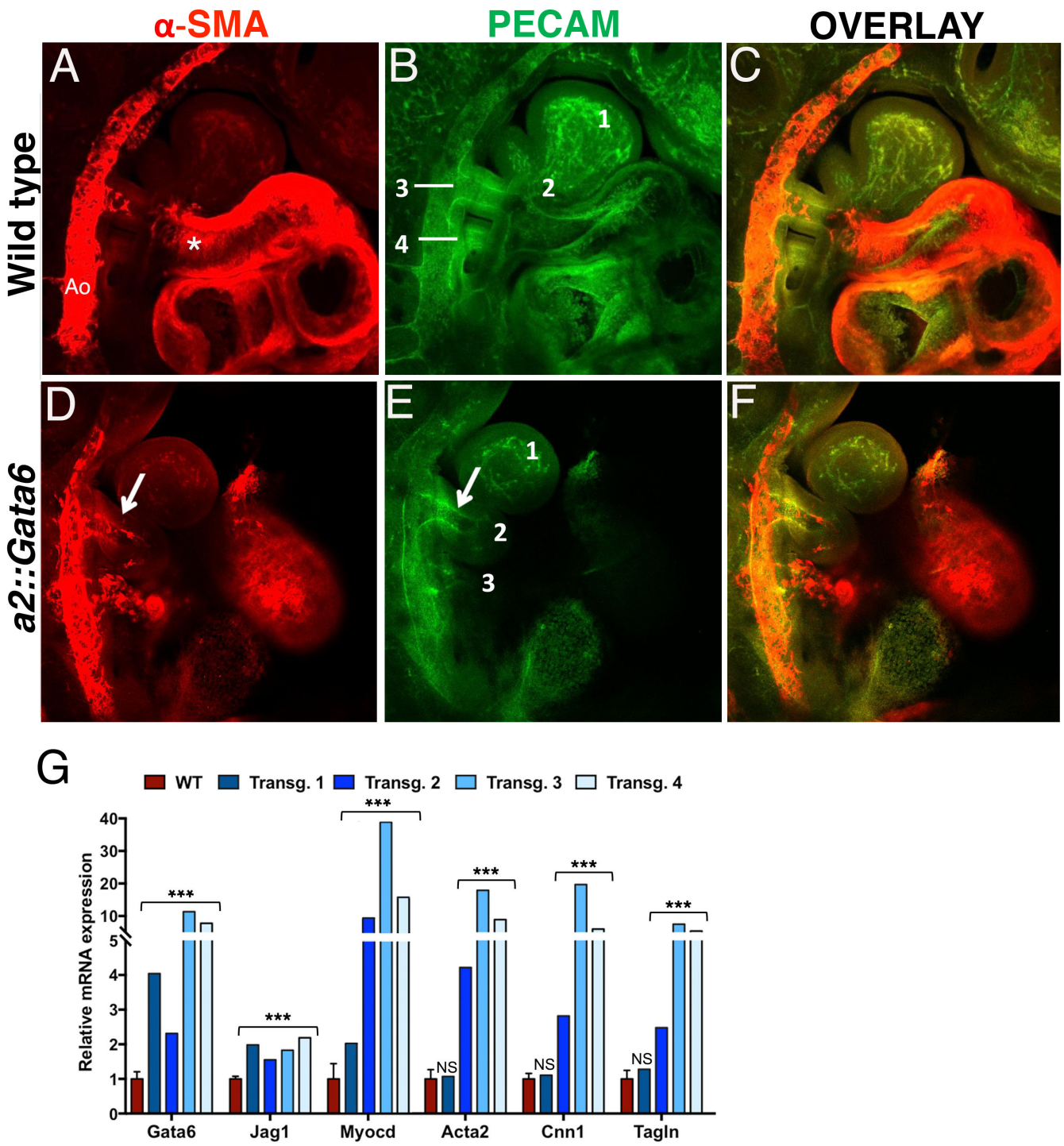

Figure 5. Gata6 is sufficient to induce SMCs in BA2 and to preserve AA2. Confocal analysis of whole mount wild type (**A–C**) and *a2::Gata6* transgenic mouse embryos (**D–F**) at E10.5 (s $\geq$ 32) to visualize vascular SMCs (a-SMA, red) (**A, D**), the endothelial network (PECAM, green) (**B, E**) and SMA/PECAM overlay (**C, F**); see also ***Figure 5—videos 1–4***. (**A-C**) In wild-type embryos, SMA-positive cells are visible in the AA3, the dorsal aorta and the heart, but are not detected in BA2, where AA2 has regressed to a capillary bed (see also ***Figure 2***). D-F, In *a2::Gata6* embryos, vascular SMCs are detected in the BA2 (arrows in D). In the majority of transgenic embryos analyzed, the BA2 hosts a persistent artery connected to the heart (arrow in E). For best

Figure 5 continued on next page

Figure 5 continued

visualization of the ectopic AA2, an individual z-stack is shown in (**D–F**); the complete z-stack series is shown in ***Figure 5—videos 3–4***. (**G**) Quantitative RT-PCR analysis of changes in gene expression in *a::Gata6* embryos (s $\geq$ 37) and littermate controls. The wild-type values are presented as a mean ± SEM of two technical replicates of four independent embryos. For each transgenic embryo, the average of two technical replicates ± SEM is shown. Transgenic embryos 2–4 showed evidence of a functional AA2. Conversely, transgenic embryo one did not show significant upregulation of SMC-markers relative to wild-type; this embryo had no evidence of ectopic AA2. Asterisks (***) correspond to pvalues < 0.005; NS = not significant. All the results of transgenic embryos analyses are summarized in ***Figure 5—source data 1***. Ao, dorsal aorta; numbers indicate BAs and corresponding AAs. Asterisks label the OFT.

DOI: https://doi.org/10.7554/eLife.31362.010

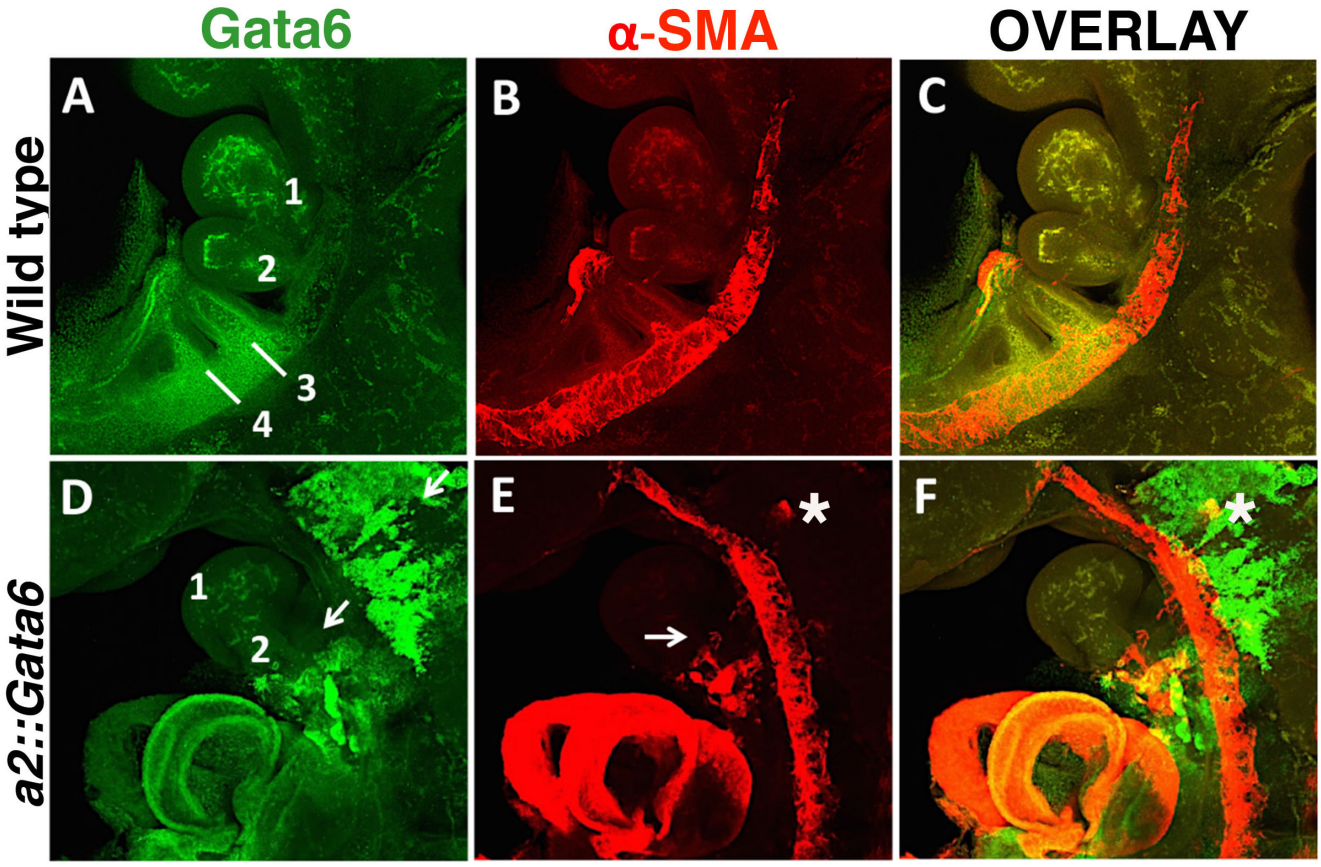

Figure 5—figure supplement 1. Gata6 ectopic expression in *a2::Gata6* embryos. Confocal analysis of whole mount wild type (**A–C**) and a2::Gata6 embryos (**D–F**) at E10.5 to visualize Gata6 (**A**, **D**, green) and VSMCs (**C**, **E** a-SMA, red) and Gata6/SMA overlay (**C**, **F**). (**A–C**) High levels of Gata6 are detected in the PBAs (see also ***Figure 3G***). SMA-positive cells are visible in the AA3, the dorsal aorta and the heart, but are not detected in BA2. (**D–F**) Expression of Gata6 in the NC migrating to the BAs (arrow), in BA2 (2, arrow) and in PBAs in *a2::Gata6* transgenic embryos. Ectopic SMCs were exclusively detected in transgenic embryos displaying Gata6 overexpression. Gata6 expression largely overlaps with SMA staining in the aortic arches of transgenic embryos. A cluster of Gata6-positive, SMA-positive cells is observed along NC migration route (asterisk).

DOI: https://doi.org/10.7554/eLife.31362.011

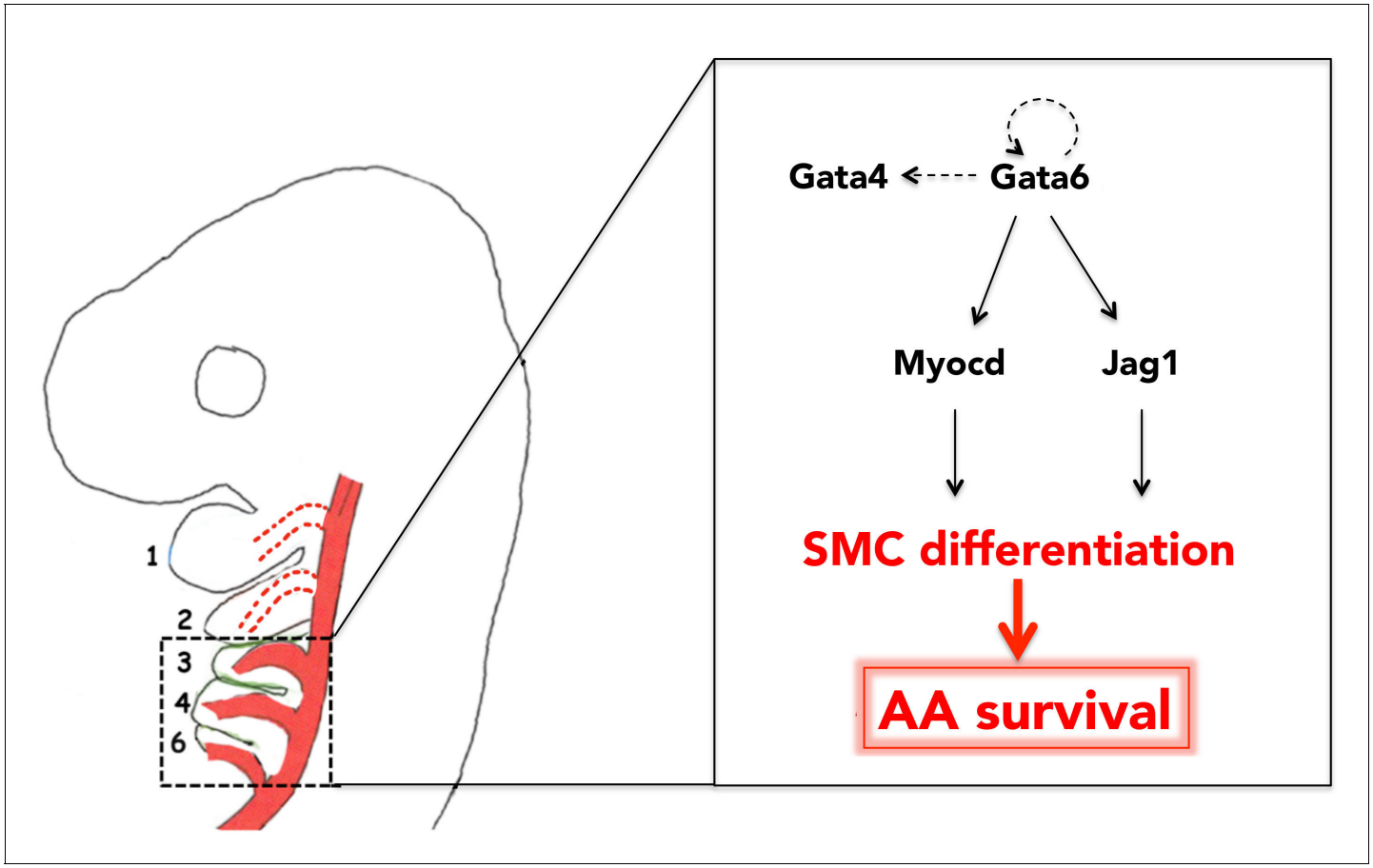

Figure 6. Gata6-driven SMC differentiation promotes survival of the posterior AAs. Gata6 activates *Myocd* and *Jag1* to initiate SMC differentiation in the cardiac NC, migrating to BA3-6. Generation of SMCs in BA3-6, and their recruitment by AA3-6, results in the stabilization of these vessels and their subsequent incorporation into the mature aortic tree. Conversely, because Gata6 is not expressed in BA1-2, AA1-2 do not 'see' any SMC and eventually regress. Auto-regulatory loops involving GATA TFs are likely features of Gata6 network. Arrows and double arrow indicate regulation and interaction, respectively; broken arrows indicate links that are not experimentally validated.

DOI: https://doi.org/10.7554/eLife.31362.018